Biomaterials 31 (2010) 900–907

Contents lists available at ScienceDirect

Biomaterials

journal homepage: www.elsevier.com/locate/biomaterials

The role of antibody synergy and membrane fluidity in the vascular targeting of immunoliposomes

Rico C. Gunawan, Debra T. Auguste*

School of Engineering and Applied Sciences, Harvard University, 29 Oxford St., Cambridge, MA 02138, USA

ARTICLE INFO

Article history:
Received 18 August 2009
Accepted 29 September 2009
Available online 30 October 2009

Keywords:
Immunoliposome
Membrane elasticity
Cell adhesion molecule
Endocytosis
Synergy
Mobility

ABSTRACT

Targeted drug delivery to inflamed or injured vascular endothelial cells (ECs) and smooth muscle cells (SMCs) may provide a precise and effective therapeutic treatment for cardiovascular diseases. Upregulation of cytokine-regulated cell surface receptors, intercellular cell adhesion molecule-1 (ICAM) and endothelial-leukocyte adhesion molecule-1 (ELAM), on ECs and SMCs are used to target drug delivery vehicles. Recent studies demonstrate clustering of these molecules in lipid rafts may affect binding due to a nonhomogenous presentation of antibodies. We hypothesized that altering the antibody ratio for ICAM and ELAM (aICAM:aELAM) and mobility would influence cellular targeting. To alter antibody mobility, liposomes were prepared from either 1,2-dioleoyl-sn-glycero-3-phosphatidylcholine (DOPC, $C_{18:1}$, $T_m = -20\,^{\circ}C$) or 1,2-dipalmitoyl-sn-glycero-3-phosphatidylcholine (DPPC, $C_{16:0}$, $T_m = 42\,^{\circ}C$) which are in the liquid crystalline (L_α) and gel phase (L_β) at 37 °C, respectively. We report that cellular binding of DOPC immunoliposomes by ECs is maximal at an equimolar ratio of aICAM:aELAM whereas DPPC immunoliposomes showed no ratio dependence and binding was reduced by more than 2-fold. SMCs, which do not express ELAM, show a dependence on aICAM surface density. These results suggest that antibody mobility and molar ratio play a key role in increasing receptor-mediated cell targeting.

© 2009 Elsevier Ltd. All rights reserved.

1. Introduction

The endothelial lining of the cardiovascular system undergoes cytokine [1] and/or shear-induced [2] activation during acute and chronic inflammation, injury and repair, angiogenesis, and atherogenesis [3]. Localized endothelial activation is marked by an increase in cell surface expression of adhesion molecules such as endothelial-leukocyte adhesion molecule-1 (ELAM), vascular cell adhesion molecule-1 (VCAM), and intercellular adhesion molecule-1 (ICAM) [4,5]. Human umbilical vein endothelial cells activated by a pro-inflammatory stimuli, such as the cytokine interleukin-1α (IL-1α), upregulate expression of ELAM-1, VCAM-1, and ICAM-1 in temporally well characterized patterns, providing a useful in vitro model system that mimics EC activation [6,7].

Targeting the vascular system as a therapeutic strategy has been a primary focus in cancer [8], inflammation [9], and ischemia [9]. One strategy utilizes the increased expression of specific adhesion molecules to facilitate the delivery of therapeutic agents to activated ECs. Nanocarriers modified with either anti-ELAM (aELAM) [3], anti-VCAM [10], and anti-ICAM (aICAM) [11,12] have shown selectivity for activated ECs. Transiently-upregulated cell adhesion molecules on ECs enhance binding and uptake of drug delivery vehicles when presenting a single targeting ligand.

Antibodies may work synergistically to target cells effectively. Targeting using two different antibodies has increased binding specificity and cellular uptake of liposomes in comparison to liposomes with only one antibody [13]. Adhesion of microspheres coated with aICAM and sialyl Lewis^x, a selectin ligand, showed a concentration dependence of both ligands [14,15]. In addition, clustering of ELAM and ICAM on the EC surface during leukocyte adhesion has been implicated in protein trafficking and signal transduction [16]. The relationship between one or more antibodies and antibody surface presentation (e.g. neighboring distance, orientation) to optimize EC binding and uptake remains unknown.

Immunoliposomes are concentric bilayers of lipid surrounding an aqueous core that target a specific cell type by presenting molecules that bind to antigens on the cell surface. Liposomal drug delivery vehicles offer several advantages due to their structural versatility related to size, composition, bilayer fluidity, and ability to encapsulate a large variety of compounds non-covalently [17]. Liposomes are capable of delivering drugs or genes to cells or tissues (e.g., stealth liposomes with a polyethylene-glycol (PEG) coat [18], pH-sensitive liposomes [19], cationic liposomes [20], fusogenic protein-conjugated liposomes [21], target sensitive

* Corresponding author. Tel.: +1 617 384 7980; fax: +1 617 495 9837.
E-mail address: auguste@seas.harvard.edu (D.T. Auguste).

0142-9612/$ – see front matter © 2009 Elsevier Ltd. All rights reserved.
doi:10.1016/j.biomaterials.2009.09.107

liposomes [22], and immunoliposomes [10]). In addition, liposomes are often assembled from lipids that are mobile on the surface which offers another degree of freedom unlike nanoparticles which have immobile, covalently-conjugated targeting moieties.

ELAM and ICAM have been shown to cluster following their engagement in a cytokine or shear-induced response [16]. Clustering of ELAM at the lipid surface is required for subsequent cell signaling and gene expression [23]. While numerous studies have reported that receptor mobility and clustering affect cell-membrane adhesion [24–26], no studies have been reported for liposome-cell binding. We hypothesize that the mobility of the lipid carrier will affect the distribution of cell receptors on the liposome to compliment the natural arrangement of its antigen on the cell surface and facilitate clustering and downstream signaling.

Liposomes composed of lipids with differing chain length and degree of saturation were used to alter antibody mobility. DPPC is saturated; it has a C16 acyl chain that packs tightly and forms a gel below its melting temperature, $T_m = 42\,^{\circ}C$. DOPC is unsaturated, having a cis double bond (Δ9) in each C18 chain. DOPC lipids are mobile above $T_m = -20\,^{\circ}C$. Differences in the dynamic surface elasticity and dilational viscosity of DPPC and DOPC monolayers have been reported [27]. In addition, the effect of temperature on DOPC and DPPC monolayers has been studied by atomic force microscopy which yields differences in elastic properties and bilayer thickness [28]. Surface rheology of DPPC and DOPC lipid monolayers at the air–water interface reveal a transition between the liquid expanded to liquid condensed phase at 60 and 100 $Å^2$ per molecule, respectively [29].

Here, we report the effect of antibody mobility on immunoliposomes bearing two distinct antibodies (aICAM and aELAM) expressed on ECs and SMCs. Immunoliposomes were designed to target ICAM and ELAM receptors by simultaneous conjugation of aICAM and aELAM on lipids via N-hydroxysuccinimide/N-ethyl-N′-(3-dimethylaminopropyl)carbodiimide (NHS/EDC) chemistry (Fig. 1A). Their in vitro binding to ECs and SMCs expressing ICAM and ELAM were characterized and evaluated using flow cytometry and immunofluorescent staining.

2. Experimental methods

2.1. Materials

1,2-dioleoyl-sn-glycero-3-phosphoethanolamine-N-dodecanoyl (N-dod-PE), 1,2-dioleoyl-sn-glycero-3-phosphocholine (DOPC), and 1,2-dipalmitoyl-sn-glycero-3-phosphocholine (DPPC) were purchased from Avanti Polar Lipids (Alabaster, AL). Interleukin-1α (IL-1α), mouse anti-human ICAM, mouse anti-human ELAM monoclonal antibodies (mAbs), and IgG_1 isotype (mAb) were purchased from R&D Systems (Minneapolis, MN). EDC, NHS, Triton X-100, bovine serum albumin (BSA), human fibronectin, rhodamine-B isothio-cyanate-conjugated dextran (10 kDa MW), ammonium molybdate, ascorbic acid, anhydrous dimethyl sulfoxide (DMSO), and ethanol (EtOH) were purchased from Sigma (St. Louis, MO). Formaldehyde was obtained from EMD Chemicals, Inc. (Gibbstown, NJ). FITC-conjugated goat anti-mouse, TRITC-conjugated sheep anti-mouse, and rabbit anti-sheep secondary antibodies were obtained from Abcam (Cambridge, MA). Sheep anti-human ELAM polyclonal antibodies were purchased from Leinco Technologies (St. Louis, MO). Dulbecco's phosphate buffered saline (PBS), 0.25% trypsin/2.6 mM EDTA, Hoechst 33258, L-glutamine, penicillin/streptomycin (pen-strep), and ITS (insulin, transferrin, and selenium) solution were obtained from Invitrogen (Carlsbad, CA). Primers (ICAM: Hs00164932_m1, ELAM: Hs00174057_m1, GAPDH: Hs02758991_g1) and reagents for quantitative reverse transcriptase polymerase chain reaction (qRT-PCR) were procured from Applied Biosystems (Foster City, CA).

2.2. Liposome preparation

Unilamellar liposomes were prepared by the extrusion method according to Szoka [30]. A mixture of DOPC:N-dod-PE or DPPC:N-dod-PE (95:5 mol%) in chloroform was dried in a rotary evaporator under reduced pressure. The lipids were then dissolved in a mixture of DMSO:EtOH (7:3 v/v). Lipid mixtures (0.3 ml) were injected in 3 ml PBS (pH 7.4) with or without rhodamine-conjugated dextran (1 mg/ml) while being agitated at 650 rpm with a stir bar to yield 50 mM lipid. DPPC mixture was heated to 50 °C during the extrusion. Dextran-encapsulated liposomes

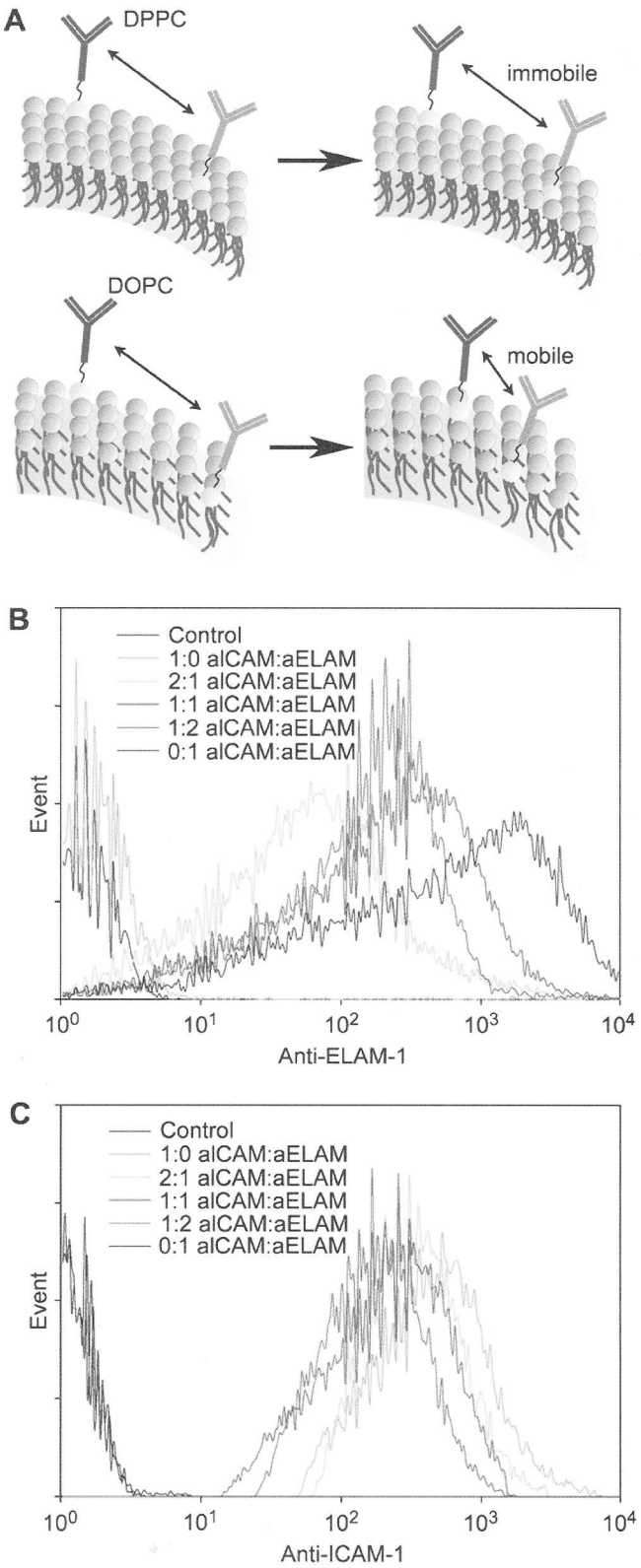

Fig. 1. Immunoliposomes conjugated with different aICAM:aELAM molecules. aICAM and aELAM on DPPC:N-dod-PE immunoliposomes are immobile while those on DOPC immunoliposomes are mobile at 37 °C (A). Fluorescence histograms of 2-micron borosilicate beads coated with DPPC:N-dod-PE (95:5 mol:mol) liposomes conjugated with aICAM and aELAM antibodies with aICAM:aELAM molar ratios of 1:0, 2:1, 1:1, 1:2, and 0:1. Fluorescence intensities correlate with the antibody molar ratios for both aELAM (B) and aICAM (C).

were dialyzed against PBS using a Slide-A-Lyzer dialysis cassette (MWCO 20 kDa, Pierce Biotechnology, Inc., Rockford, IL) overnight at room temperature (RT). Liposome size and zeta potential were measured by dynamic light scattering on a Zeta-PALS analyzer (Brookhaven Instruments, Corp., Holtsville, NY) in PBS (pH 7.4).

The concentration of lipid in solution was determined by a phosphate assay as previously described [31]. Briefly, a diluted liposome sample was ashed with 0.2 ml sulfuric acid (10% v/v) at 200 °C for 1 h, followed by addition of 50 μl hydrogen peroxide (30% v/v) and further heating at 200 °C for 40 min. After the sample was cooled down to RT, 480 ml deionized water and 0.5 ml of colour reagent (0.5% w/v ammonium molybdate, 2% w/v ascorbic acid) were added to each sample followed by heating at 45 °C for 20 min. The samples were read at 820 nm using a Spectramax Plus 384 spectrophotometer (Molecular Devices, Sunnyvale, CA).

2.3. Preparation of antibody-labeled liposomes and microspheres

Antibodies were conjugated to liposomes via the N-dod-PE anchor. EDC (2 mg) and NHS (3 mg) were added to 1 μmol lipid (liposomes) in PBS (pH 7.4) and incubated for 6 h at RT. Excess EDC and NHS were removed using the Zeba Spin desalting column (MWCO 7 kDa, Pierce Biotechnology, Inc.). IgG_1 isotype (100 mol%, unspecific liposome) or mixtures of aICAM:aELAM (1:0, 0:1, 2:1, 1:1, and 1:2 molar ratios) were added to EDC-modified liposomes at a molar ratio of 1:1000 antibody:phospholipids and incubated overnight at RT. Free antibodies were separated using a Sepharose CL-4B column (Fractionation range: 60–20,000 kDa, Sigma).

To determine antibody density of aICAM and aELAM, 2-micron borosilicate beads (Duke Scientific, Palo Alto, CA) were immersed in PC:N-dod-PE (95:5) liposomes in PBS and agitated for 6 h. Microbeads were washed 3 times with PBS through centrifugation–suspension cycles to separate free liposomes. Conjugation of different ratios of aICAM:aELAM and control IgG (nonspecific binding) to microbeads was performed as described above using EDC/NHS chemistry. After free primary antibodies were separated, microbeads were conjugated with FITC-conjugated goat anti-mouse (aELAM binding) and TRITC-conjugated rabbit anti-sheep (aICAM binding) secondary antibodies (10 μl, 10 ng/ml) overnight at 4 °C. The secondary antibodies were separated using suspension–spin cycles. The density of aELAM and aICAM conjugated to the microbeads was determined with reference to Quantum™ Simply Cellular® microbeads (Bangs Laboratory, Inc., Fishers, IN), which have defined numbers of antibody binding site per bead.

2.4. Cell culture

Human umbilical vein endothelial cells (ECs) and aortic smooth muscle cells (SMCs) were grown in endothelial growth medium-2 (EGM-2) and smooth muscle growth medium-2 (SmGM-2) media, respectively, with supplements (Lonza, Allendale, NJ). Vein ECs and aortic SMCs have been characterized widely and used commonly to study cardiovascular systems. Aortic and vein ECs show qualitatively similar growth, morphology, and response to adhesion molecule modulation [32–36]. We were unable to secure vein smooth muscle cells from Lonza and have continued our study using aortic smooth muscle cells. Cells were maintained at 37 °C in a humidified incubator with 5% CO_2 and used for experiments at passages 5–10.

2.5. ICAM immunostaining

ECs and SMCs (2×10^5 cells) were seeded on 18×18 mm^2 coverslips in 6-well plates with 2 ml media (VWR, West Chester, PA) and cultured overnight at 37 °C. Cells were incubated with IL-1α at 5 ng/ml in fresh EGM-2 media the next day for 6 h. After media was removed, cells were rinsed with PBS three times and fixed with 4% formaldehyde in PBS at RT for 15 min followed by washing with PBS. Samples were blocked with 1% BSA in PBS (1% BSA) at 4 °C for 1 h. Samples were then stained with aICAM mAbs (10 ng/ml in 1% BSA) at 4 °C for 2 h and rinsed with PBS. Samples were incubated with FITC- or TRITC-conjugated goat anti-mouse secondary mAbs (1:300) and Hoescht 33258 (1:1000) at 4 °C for 1 h followed by washing with PBS. Samples were then mounted on microscope slides (3″ × 1″, VWR) with VECTASHIELD® mounting medium (Vector Laboratories, Burlingame, CA), and sealed. Samples were examined under an Axiovert 200 inverted fluorescent microscope (Carl Zeiss, Thornwood, NY) equipped with a Hammamatsu CCD camera (Bridgewater, NJ). Digital images were captured with AxioVision digital image processing software (Zeiss).

2.6. ICAM and ELAM Expression

Expression level of ICAM and ELAM on ECs and SMCs was characterized using qRT-PCR. ECs and SMCs were cultured at 3×10^5 cells/well overnight and incubated with IL-1α for 30 min, 1 h, 6 h, 12 h, 24 h, and 48 h. After each incubation time, ECs and SMCs were removed from each well by incubating with a trypsin/EDTA solution for 3 min. The cells were washed with PBS 3 times. RNA was extracted, purified using the Qiagen RNeasy minikit (Valencia, CA), and detected by a spectrophotometer. Reverse transcription was conducted using the Applied Biosystems Taqman RT protocol. Detection and quantification of RNA was performed by the 7300 Real-Time PCR system (Applied Biosystems). All PCR samples were referenced to the gene expression of GAPDH.

Densities of ICAM and ELAM expressed by ECs and SMCs at 6 h was determined using Quantum™ Simply Cellular® microbeads and performed using the protocol as provided by the manufacturer.

2.7. Uptake of immunoliposomes by ECs and SMCs

Liposome binding by ECs and SMCs was analyzed using flow cytometry as previously described [37–39]. ECs and SMCs were seeded in 6-well plates (3×10^5 cells/well) and allowed to adhere overnight. After activation with IL-1α for 6 h, ECs and SMCs were incubated overnight at 37 °C with: (1) dextran-loaded unlabeled liposomes (DPPC:N-dod-PE, 95:5, and DOPC:N-dod-PE, 95:5); (2) dextran-loaded nonspecific (IgG) liposomes; (3) dextran-loaded immunoliposomes conjugated with different ratios of aICAM/aELAM mAb. The concentration used was 1 μmol lipid/10^6 cells.

Treated ECs or SMCs were washed with PBS, harvested using trypsin/EDTA solution, and collected in a polystyrene culture tube. Cells were washed with PBS three times. Binding data were acquired using an LSRII flow cytometry (BD Immunocytometry Systems, San Jose, CA) and analyzed with WEASEL software developed by WEHI (Parkville, Australia). The fold-over isotype value, which was calculated by dividing the mean fluorescence intensity for immunoliposomes conjugated with aICAM:aELAM by that of the isotype-conjugated liposomes, was used to normalize the data. The significant difference in liposome uptake from different samples was evaluated using a two-tailed Student's *t*-test.

Binding of liposomes by activated ECs and SMCs was also visualized by epifluorescence. After incubation with liposomes, cells were fixed and stained with aICAM mAb as previously described.

3. Results and discussion

3.1. Nanocarrier characterization

Unilamellar DOPC:N-dod-PE (95:5) and DPPC:N-dod-PE (95:5) liposomes were prepared by the extrusion method. Unlabeled DOPC:N-dod-PE and DPPC:N-dod-PE liposomes had diameters of 205 ± 5 nm and 201 ± 4 nm, respectively, as determined from dynamic light scattering. The diameter of immunoliposomes with bound aICAM and aELAM were similar for all antibody ratios (223 ± 3 nm for DOPC and 219 ± 7 nm for DPPC). The average antibody density determined from the standardized microbeads was 1746 ± 60 molecules/μm^2 or 123 ± 5 molecules/liposome. The size and surface charge of both DOPC and DPPC immunoliposomes were similar at all tested ratios (Table 1). To confirm conjugation of different molar ratios of aICAM and aELAM, 2-micron borosilicate beads were coated with DOPC:N-dod-PE (95:5) and DPPC:N-dod-PE liposomes and labeled with antibodies, aICAM and aELAM, by conjugating with EDC/NHS. Flow cytometry analysis of the fluorescence intensities of aICAM and aELAM conjugated to DPPC:N-dod-PE on beads using fluorescently-labeled secondary antibodies showed that the fluorescence intensity shifted as the aICAM:aELAM ratio was increased (Fig. 1B, C). The amount of aELAM and aICAM on the surface was quantified using reference beads of known density (Table 1). Flow cytometry analysis of antibody bound to DOPC:N-dod-PE liposomes was similar to DPPC:N-dod-PE. The surface density of 5 mol% N-dod-PE was chosen based on preliminary experiments that showed no change in binding between 5 and 10 mol% N-dod-PE. This antibody to lipid ratio is similar to other reports [40,41].

Table 1
Antibody density and zeta potential of DPPC:N-dod-PE immunoliposomes.

Ratio aICAM:aELAM	aICAM (molecules/μm^2)	aELAM (molecules/μm^2)	Zeta potential (mV)
1:0	1786 ± 87	–	1.1 ± 0.4
2:1	1252 ± 123	554 ± 39	0.8 ± 0.5
1:1	832 ± 85	836 ± 30	1.6 ± 0.6
1:2	586 ± 93	1111 ± 155	0.7 ± 0.3
0:1	–	1773 ± 115	1.2 ± 0.4

3.2. ICAM and ELAM expression on ECs and SMCs

IL-1α has been shown to upregulate the expression of ICAM and ELAM on ECs [5]. ECs were activated with 5 ng/ml IL-1α for different time intervals from 1 to 48 h. As determined from qRT-PCR, the expression levels of both ICAM and ELAM increased with exposure time and reached a maximum at 6 h, 70-fold and 200-fold, respectively, greater than the levels for non-activated ECs (Fig. 2A). At 48 h, ICAM and ELAM expression on ECs was similar to the 1 h activation although still greater than non-activated cells. SMCs showed an increase of ICAM only; there was no presence of ELAM (Fig. 2B). ICAM expression on SMCs also peaked at 6 h. The densities of ICAM and ELAM expressed by ECs and SMCs at 6 h are given in Table 2. In contrast to qRT-PCR results, the density of ICAM increased by 15-fold on activated ECs and 2-fold on activated SMCs. Expression of ELAM increased by 5-fold on ECs while it remained constant on activated SMCs. Based on these data, further experiments were performed on ECs and SMCs after a 6-h activation with IL-1α.

Our time-course expression of ICAM and ELAM agrees with literature. ELAM expression on ECs has been shown to be expressed transiently with a peak observed at 4–6 h after activation with cytokines [33,42,43]. However, our ICAM expression plateaued faster on ECs than what was observed previously (ca. 12–24 h) [33]. This difference can be attributed to variation in cell sources and cytokine concentrations used. As anticipated, activated SMCs only expressed ICAM [35].

Temporal and spatial expression of ICAM and ELAM on ECs and SMCs can be explained from the role of these adhesion molecules in the inflammatory response. ELAMs initiate leukocyte rolling on endothelium in response to inflammatory cues such as interleukin or tumor necrosis factor prior to adhering firmly via ICAMs on ECs and transmigrating to inflamed tissues [15,44]. Thus, ELAMs were not expected to be expressed on SMCs since endothelium maintains the gatekeeping function.

3.3. Cellular binding

Cellular binding of immunoliposomes was measured by flow cytometry. Immunoliposomes encapsulating rhodamine-dextran, either bound to the cell surface or internalized, were detected. Here, we compare immunoliposome binding for activated and non-activated ECs, at various aICAM:aELAM ratios, and as a function of surface mobility (DOPC vs. DPPC). We also discuss immunoliposome binding to SMCs, which do not upregulate ELAM.

3.3.1. Activated vs. non-activated ECs

The binding of immunoliposomes by activated and non-activated ECs was analyzed as a function of aICAM to aELAM ratio on the liposome surface (Fig. 3). Increased binding of DOPC immunoliposomes relative to DPPC immunoliposomes on activated ECs was visually apparent (Fig. 3A, B). Activated ECs bound DOPC immunoliposomes up to 3-fold more than non-activated ECs. The binding level by activated ECs initially increased with decreasing aICAM:aELAM molar ratio, eventually reaching a maximal level at 1:1 aICAM:aELAM (Fig. 3C). For instance, DOPC immunoliposome binding was approximately 4.5, 6.5, and 2.7 fold, respectively, for 2:1, 1:1, and 1:2 (aICAM:aELAM, mol:mol). In contrast, the binding level for non-activated ECs was similar for all aICAM:aELAM ratios tested.

Incorporating both aICAM and aELAM increased the cellular uptake of immunoliposomes in comparison to the uptake of individual aICAM and aELAM-labeled liposomes, suggesting that targeting both cell adhesion molecules has a synergistic effect. Activated and non-activated ECs had similar cellular binding of liposomes with only aICAM or aELAM presented on the surface, which was at most 3-fold less than having an equimolar ratio of both aICAM and aELAM. This work builds upon Kessner et al. who reported 25% internalization by activated ECs using 100% ELAM conjugated immunoliposomes (25–30 aELAM/liposome) on liposomes in the mobile, liquid crystalline phase [41]. Other work with two different antibodies, αCD19 and αCD20, also showed that binding of liposomes with mixed populations (1:1) was greater than that of either individually targeted liposomes alone [13]. Eniola et al. showed that PLGA microspheres coated with aICAM and a ligand for P-selectin adhered more firmly to a substrate when two targeting ligands were able to interact with their respective receptors during flow [14]. Thus, multiple ligands increase adhesion and specificity. We demonstrated that EC binding of DOPC immunoliposomes under static conditions was increased by optimizing the ratio of aICAM:aELAM. This may suggest that

Table 2
IL-1α stimulated expression of ICAM and ELAM on ECs and SMCs (molecules/cell).

	ECs		SMCs	
	Not activated	Activated	Not activated	Activated
ICAM	13,500 ± 2200	208,000 ± 28,000	79,300 ± 6000	198,000 ± 11,000
ELAM	37,700 ± 11,000	187,000 ± 12,000	18,400 ± 2000	20,300 ± 1600
Isotype	6700 ± 800	22,000 ± 5000	8900 ± 600	9200 ± 200

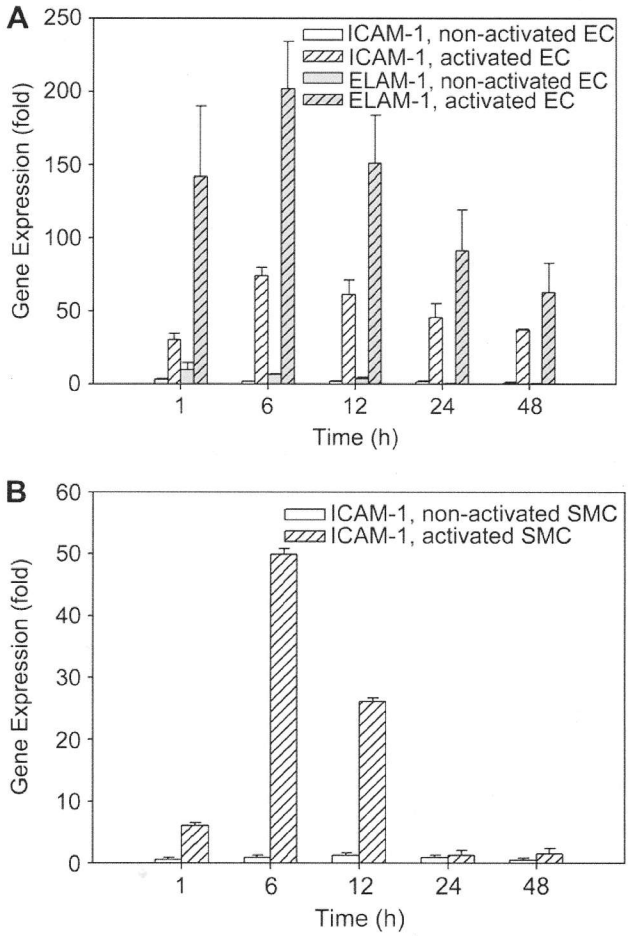

Fig. 2. ICAM and ELAM expression for IL-1α-activated ECs and SMCs. Cells were treated with IL-1α for various durations. qRT-PCR was used to analyze ICAM and ELAM expression of ECs (A) and SMCs (B). Both ICAM and ELAM expression plateaued at 6 h. SMCs only expressed ICAM.

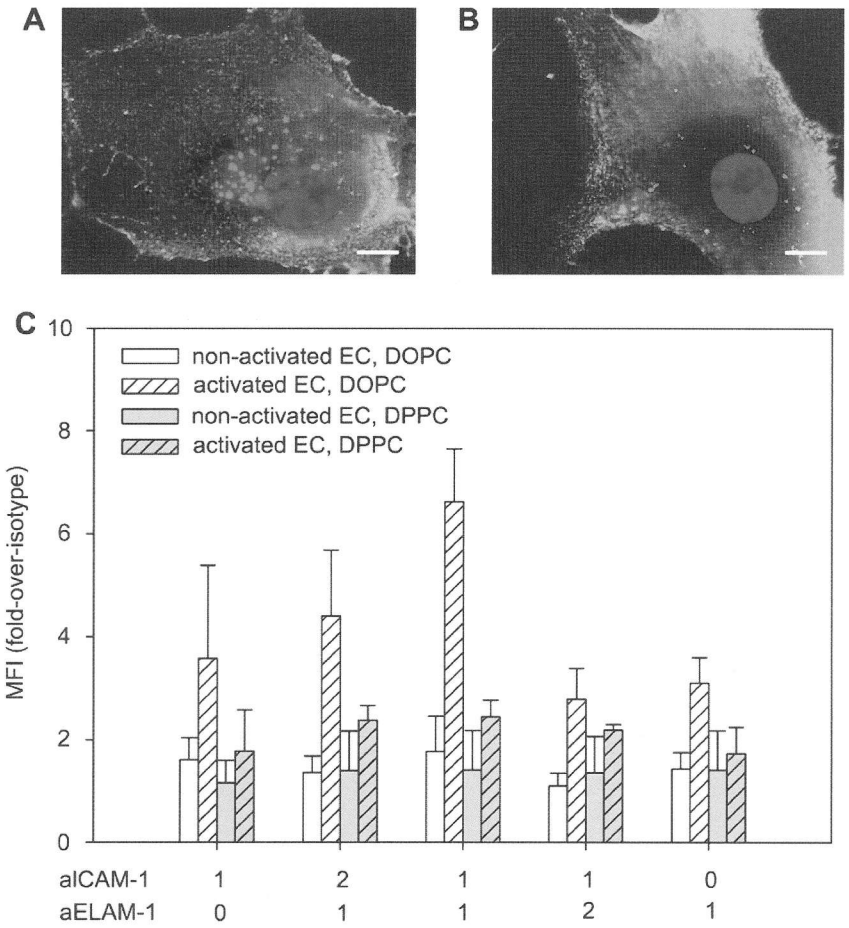

Fig. 3. Uptake of immunoliposomes by ECs. Activated ECs (IL-1α for 6 h) were treated with either rhodamine-labeled dextran encapsulated in DOPC:N-dod-PE (95:5 mol:mol) (A) or DPPC:N-dod-PE (95:5 mol:mol) (B) conjugated with 1:1 aICAM:aELAM mAbs for 12 h and stained with aICAM mAb. (C) Flow cytometry analysis of unactivated and activated ECs incubated with DOPC or DPPC immunoliposomes conjugated with various ratios of aICAM:aELAM. Results are presented relative to uptake by IgG-labeled liposomes. Bar, 10 μm.

endothelial adhesion is modulated by dual expression of surface receptors at relative concentrations [15].

Relative to the expression of ELAM and ICAM on activated ECs, we anticipated that an equimolar ratio of aICAM and aELAM would be optimal, which was confirmed by our data. It was surprising that non-activated ECs which showed a 1:2 aICAM:aELAM surface density showed no dependence on the antibody ratio, which can be explained by the lower density of ICAM and ELAM on the cellular surface.

3.3.2. Receptor mobility on ECs

The binding level of DOPC immunoliposomes was compared to that of DPPC vesicles to assess the effect of receptor mobility on cellular uptake. Activated and non-activated ECs were treated with DPPC immunoliposomes with similar ratios of aICAM:aELAM. Fig. 3B shows the representative image of EC binding of DPPC immunoliposomes with an aICAM:aELAM ratio of 1:1. The cellular binding of DPPC immunoliposomes was slightly higher for activated than non-activated ECs at all aICAM:aELAM molar ratios ($p < 0.05$, Fig. 3C). Binding increased slightly when aICAM and aELAM were both present on the liposome surface although there is no significant difference across the various formulations (aICAM:aELAM, 2:1, 1:1,1:2). Moreover, the cellular binding of DPPC immunoliposomes was 2–3-fold lower than that of DOPC immunoliposomes at all corresponding aICAM:aELAM molar ratios.

Greater EC binding of DOPC immunoliposomes than DPPC immunoliposomes may imply that the location and density of aICAM and aELAM on the drug carrier surface enables binding and subsequent internalization. Since aICAM and aELAM are attached covalently to phospholipids in a fluid bilayer (vs. the more rigid DPPC immunoliposome network), the receptors may redistribute non-uniformly to bind cooperatively with ICAM and ELAM on cell surfaces. Cooperative binding occurs when multiple weak binding results in overall strong adhesion [45]. Cooperative binding due to multivalent ICAM ligands has been found to stimulate multiple signaling pathways while monomeric ligands were not internalized by endothelium [46,47]. Muro et al. showed that ECs internalized multivalent aICAM nanocarriers by cell adhesion molecule (CAM)-mediated endocytosis which is different from other endocytic pathways such as phagocytosis, caveoli-, clathrin-mediated pathways, and macropinocytosis [12]. Molecular densification is used to regulate cellular functions; ICAM clusters activated Src and Rho kinase and induced actin stress fibers to facilitate transport to endosomes and finally lysosomes [48]. We report greater binding and internalization of DOPC immunoliposomes than DPPC immunoliposomes by ECs based on increased receptor mobility.

3.3.3. Activated vs. non-activated SMCs

We investigated whether immunoliposomes were selective to activated ECs by measuring binding for activated and non-activated SMCs. SMCs were treated with DOPC and DPPC immunoliposomes with the same aICAM:aELAM ratios as ECs. Activated SMCs bound DOPC immunoliposomes greater than DPPC immunoliposomes as

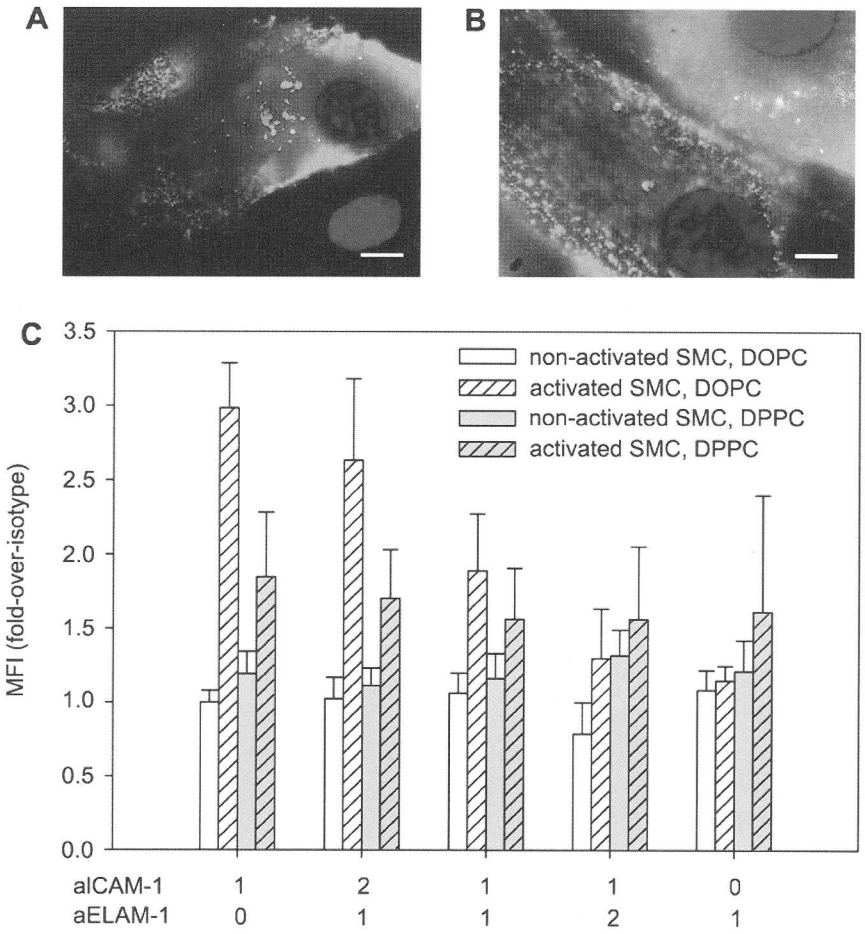

Fig. 4. Uptake of antibody-conjugated liposomes by SMCs. Activated SMCs (IL-1α for 6 h) were treated with either rhodamine-labeled dextran encapsulated in DOPC:N-dod-PE (95:5 mol:mol) (A) or DPPC:N-dod-PE (95:5 mol:mol) (B) conjugated with 1:0 aICAM:aELAM mAbs for 12 h and stained with aICAM mAbs. (C) Flow cytometry analysis of unactivated and activated SMCs incubated with DOPC:N-dod-PE or DPPC:N-dod-PE immunoliposomes conjugated with various ratios of aICAM:aELAM. Results are expressed relative to uptake by IgG-labeled liposomes. Bar, 10 μm.

shown (Fig. 4A, B). Cellular adhesion of DOPC immunoliposomes conjugated with aICAM:aELAM (1:0) was 2-fold higher for activated SMCs than non-activated SMCs (Fig. 4C), which corresponds to the doubling of ICAM molecules on activated SMCs. Increasing the molar ratio of aICAM to aELAM increased cellular binding of DOPC immunoliposomes monotonically with a maximum observed at 1:0, aICAM:aELAM. Thus, an increased surface density of aICAM increases binding. The SMC binding level for DOPC immunoliposomes conjugated with 100 mol% ICAM was 3-fold greater than at 100 mol% ELAM, equivalent to nonspecific binding. The cellular adhesion of DPPC immunoliposomes was similar for both activated and non-activated SMCs for all liposomal formulations ($p < 0.05$, Fig. 4C). DOPC immunoliposomes (1:0 aICAM:aELAM) bound activated SMCs 2-fold higher than DPPC immunoliposomes (1:0, aICAM:aELAM).

ICAM has the capacity to recycle to the cell surface after internalization. ICAM has been shown to participate in multiple rounds of binding and internalization of aICAM-conjugated nanocarriers [48]. Thus, increasing the density of aICAM on the nanocarrier surface improves cellular uptake of immunoliposomes by SMCs.

3.4. Antibody synergy and receptor mobility

The efficiency of targeting ECs increases by optimizing the ratio of two molecules, aICAM and aELAM. Activated ECs bound more than twice the number of immunoliposomes at its optimal ratio of aICAM:aELAM (1:1, max binding ratio) than activated SMCs at its optimal ratio of aICAM:aELAM (1:0, max binding ratio). The two molecules aICAM and aELAM work synergistically to increase EC binding.

We have also shown that receptor mobility is a key factor in EC targeting. DOPC and DPPC immunoliposomes differ by a single double bond and carbon tail length. In addition, the liposomes are in different phases, liquid crystalline and gel, at 37 °C. If these differences were the controlling parameters in cell binding then we would not measure differences as a function of antibody density or antibody ratio. We would also expect to observe differences in nonspecific binding which is not the case. Thus, we can conclude that the data shown arise from differences in antibody ratio and receptor mobility.

Clustering of ELAM and ICAM has been shown to mediate adhesion and translocation of leukocytes. Yang et al. reported that cross-linking ICAM induced cytoskeletal remodeling and decreased ICAM mobility [49]. ICAM clustering and translocation to caveola- and F-actin rich domains has also been shown to link the sequential steps of lymphocyte adhesion and transendothelial migration [50]. Similar to ICAM, clustering and internalization of ELAM in clathrin-coated pits enhanced ELAM's ability to mediate leukocyte rolling under flow [51]. Thus, the mobility of aICAM and aELAM on liposomes may enable clustering, which coordinates with clustering of ICAM and ELAM on EC surfaces and, hence, increases its binding and internalization.

The approach to study the role of mobility of surface receptors on cellular binding by restricting antibody movement on the liposome surface can be achieved physically by choosing lipids (DOPC vs. DPPC) with different melting temperatures as we have done here. Lipids containing diacetylene groups can be polymerized, and hence, restrict the movement of the conjugated antibody [52]. Alternatively, the fluidity of DOPC membranes can be altered modestly by adding cholesterol [53].

Our strategy does not predict the pattern of how aICAM and aELAM are distributed on the liposome surface which is an area of further investigation. Instead, we have identified that a homogeneous distribution of two antibodies has less binding than when two antibodies are able to rearrange themselves. This strategy attempts to mimic what happens naturally during interactions between cellular membranes.

4. Conclusions

By conjugating liposomes with dual antibodies, aICAM and aELAM, we have developed a drug delivery vehicle that utilizes antibody synergy to enhance binding. We showed that cellular binding of immunoliposomes could be tailored by incorporating cell adhesion molecules that are transiently upregulated on the endothelial surface. In addition, we demonstrate that cooperative binding plays a role in targeting ECs, which is enabled by antibody mobility. This targeting approach may be an effective therapy for cardiovascular diseases.

Acknowledgement

This project was supported by the Office of Naval Research (N000140710873). The authors would like to thank Andrew Wong for technical research support.

References

[1] Combe C, Duplaa C, Couffinhal T, Moreau C, Bonnet J. Induction of intercellular-adhesion molecule-1 by monocyte adhesion to endothelial-cells in human culture system. J Cell Physiol 1995;164:295–303.
[2] Andrews RK, Lopez JA, Berndt MC. Molecular mechanisms of platelet adhesion and activation. Int J Biochem Cell Biol 1997;29:91–105.
[3] Spragg DD, Alford DR, Greferath R, Larsen CE, Lee K-D, Gurtner GC, et al. Immunotargeting of liposomes to activated vascular endothelial cells: a strategy for site-selective delivery in the cardiovascular system. Proc Natl Acad Sci U S A 1997;94:8795–800.
[4] Haraldsen G, Kvale D, Lien B, Farstad IN, Brandtzaeg P. Cytokine-regulated expression of E-selectin, intracellular adhesion molecule-1 (ICAM-1), and vascular adhesion molecule-1 (VCAM-1) in human intestinal microvascular endothelial cells. J Immunol 1996;156:2558–65.
[5] Springer TA. Traffic signals on endothelium for lymphocyte recirculation and leukocyte emigration. Annu Rev Physiol 1995;57:827–72.
[6] Bevilacqua MP, Pober JS, Mendrick DL, Cotran RS, Gimbrone Jr MA. Identification of an inducible endothelial-leukocyte adhesion molecule. Proc Natl Acad Sci U S A 1987;84:9238–42.
[7] Pober JS, Bevilacqua MP, Mendrick DL, Lapierre LA, Fiers W, Gimbrone Jr MA. Two distinct monokines, interleukin 1 and tumor necrosis factor, each independently induce biosynthesis and transient expression of the same antigen on the surface of cultured human vascular endothelial cells. J Immunol 1986;136:1680–7.
[8] Heath VL, Bicknell R. Anticancer strategies involving the vasculature. Nat Rev Clin Oncol 2009;6:395–404.
[9] Simone E, Ding BS, Muzykantov V. Targeted delivery of therapeutics to endothelium. Cell Tissue Res 2009;335:283–300.
[10] Voinea M, Manduteanu I, Dragomir E, Capraru M, Simionescu M. Immunoliposomes directed towards VCAM-1 interact specifically with activated endothelial cells – a potential tool for specific drug delivery. Pharm Res 2005;22(11):1906–17.
[11] Villanueva FS, Jankowski RJ, Klibanov S, Pina ML, Alber SM, Watkins SC, et al. Microbubbles targeted to intercellular adhesion molecule-1 bind to activated coronary artery endothelial cells. Circulation 1998;98:1–5.
[12] Muro S, Wiewrodt R, Thomas A, Koniaris L, Albelda SM, Muzykantov VR, et al. A novel endocytic pathway induced by clustering endothelial ICAM-1 or PECAM-1. J Cell Sci 2003;116:1599–609.
[13] Laginha K, Mumbengegwi D, Allen T. Liposomes targeted via two different antibodies: assay, B-cell binding and cytotoxity. Biochim Biophys Acta 2005;1711:25–32.
[14] Eniola AO, Hammer DA. In vitro characterization of leukocyte mimetic for targeting therapeutics to the endothelium using two receptors. Biomaterials 2005;26:7136–44.
[15] Eniola AO, Willcox JP, Hammer DA. Interplay between rolling and firm adhesion elucidated with a cell-free system engineered with two distinct receptor-ligand pairs. Biophys J 2003;85:2720–31.
[16] Tilghman RW, Hoover RL. E-selectin and ICAM-1 are incorporated into detergent-insoluble membrane domains following clustering in endothelial cells. FEBS Lett 2002;525:83–7.
[17] Voinea M, Simionescu M. Designing of intelligent liposomes for efficient delivery of drugs. J Cell Mol Med 2002;6:465–74.
[18] Woodle MC, Newman L, Collins L, Redermann C, Martin F. Improved long circulating liposomes using synthetic lipids. Proc Int Symp Control Rel Bioact Mater 1990;17:77–8.
[19] Auguste DT, Furman K, Wong A, Fuller J, Armes SP, Deming TJ, et al. Triggered release of siRNA from poly(ethylene glycol)-protected, pH-dependent liposomes. J Control Release 2008;130:266–74.
[20] Cortesi R, Marastoni M, Tomatis R, Nienegatti E, Esposito E, Nastruzzi C. Peptide-based cationic molecules for the production of positive charged liposomes and micelles. J Microencapsul 2008;25:71–81.
[21] Kaneda Y, Uchida T, Ishiura M, Okada Y. The improved efficient method for introducing macromolecules into cells using HVJ liposomes with gangliosides. Exp Cell Res 1987;173:56–69.
[22] Ho RJY, Rouse BT, Huang L. Target-sensitive immunoliposomes, preparation and characterization. Biochemistry 1986;25:5500–6.
[23] Kiely J-M, Hu Y, Garcia-Cardena G, Gimbrone JMA. Lipid raft localization of cell surface E-selectin is required for ligation-induced activation of phospholipase Cγ. J Immunol 2003;171:3216–24.
[24] Garcia AS, Dellatore SM, Messersmith PB, Miller WM. Effects of supported lipid monolayer fluidity on the adhesion of hematopoietic progenitor cell lines to fibronectin-derived peptide ligands for α5β1 and α4β1 integrins. Langmuir 2009;25:2994–3002.
[25] Nam J-M, Nair PM, Neve RM, Gray JW, Groves JT. A fluid membrane-based soluble ligand-display system for live-cell assays. Chembiochem 2006;7:436–40.
[26] Chan P-Y, Lawrence MB, Dustin ML, Ferguson LM, Golan DE, Springer TA. Influence of receptor lateral mobility on adhesion strengthening between membranes containing LFA-3 and CD2. J Cell Biol 1991;115:245–55.
[27] Vrânceanu M, Winkler K, Nirschl H, Leneweit G. Surface rheology and phase transitions of monolayers of phospholipid/cholesterol mixtures. Biophys J 2008;94:3924–34.
[28] Leonenko ZV, Finot E, Ma H, Dahms TES, Cramb DT. Investigation of temperature-induced phase transitions in DOPC and DPPC phospholipid bilayers using temperature-controlled scanning force microscopy. Biophys J 2004;86:3783–93.
[29] Yan W, Piknova B, Hall SB. The collapse of monolayers containing pulmonary surfactant phospholipids is kinetically determined. Biophys J 2005;89:306–14.
[30] Szoka JFC, inventor. The regents of the University of California, assignee. Preparation of liposome and lipid complex compositions. USA, 1996.
[31] Itoh YH, Itoh T, Kaneko H. Modified Bartlett assay for microscale lipid phosphorus analysis. Anal Biochem 1986;154:200–4.
[32] Cartwright JE, Whitley GSJ, Johnstone AP. The expression and release of adhesion molecules by human endothelial cell lines and their consequent binding of lymphocytes. Exp Cell Res 1995;217:329–35.
[33] Pober JS, Cotran RS. Cytokines and endothelial cell biology. Physiol Rev 1990;70:427–51.
[34] Tummala PE, Chen XL, Medford RM. NF-kappa B independent suppression of endothelial vascular cell adhesion molecule-1 and intercellular adhesion molecule-1 gene expression by inhibition of flavin binding proteins and superoxide production. J Mol Cell Cardiol 2000;32:1499–508.
[35] Wang X, Feuerstein GZ, Gu J-L, Lysko PG, Yue T-L. Interleukin-1β induces expression of adhesion molecules in human vascular smooth muscle cells and enhances adhesion of leukocytes to smooth muscle cells. Atherosclerosis 1995;115:89–98.
[36] Wright PS, Cooper JR, Kropp KE, Busch SJ. Induction of vascular cell adhesion molecule-1 expression by IL-4 in human aortic smooth muscle cells is not associated with increased nuclear NF-kappa B levels. J Cell Physiol 1999;180:381–9.
[37] Marty C, Meylan C, Schott H, Ballmer-Hofer K, Schwendener RA. Enhanced heparan sulfate proteoglycan-mediated uptake of cell-penetrating peptide-modified liposomes. Cell Mol Life Sci 2004;61:1785–94.
[38] Curtsinger JC, Deeths MJ, Pease P, Mescher MF. Artificial cell surface constructs for studying receptor–ligand contributions to lymphocyte activation. J Immunol Methods 1997;209:47–57.
[39] Kerby MB, Urban JC, Mouallem L, Tripathi A. Circulating IgSF proteins inhibit adhesion of antibody targeted microspheres to endothelial inflammatory ligands. Appl Biochem Biotechnol 13 January 2009. Online First™.
[40] Kung VT, Redemann CT. Synthesis of carboyxacyl derivatives of phophatidylethanolamine and use as an efficient method for conjugation of protein to liposomes. Biochim Biophys Acta 1986;862:435–9.
[41] Kessner S, Krause A, Rothe U, Bendas G. Investigation of the cellular uptake of E-selectin-targeted immunoliposomes by activated human endothelial cells. Biochim Biophys Acta 2001;1514:177–90.

[42] Hussein MNA, Meesters EW, Osmanovic N, Romijn FPHTM, Nieuwland R, Sturk A. Antigenic characterization of endothelial cell-derived microparticles and their detection ex vivo. J Thromb Haemost 2003;1:2434–43.
[43] Lee KH, Lawley TJ, Xu Y, Swerlick RA. VCAM-1-, ELAM-1-, and ICAM-1-independent adhesion of melanoma cells to cultured human dermal microvascular endothelial cells. J Invest Dermatol 1992;98:79–85.
[44] Butcher EC. Leukocyte-endothelial cell recognition: three (or more) steps to specificity and diversity. Cell 1991;67:1033–6.
[45] Auguste DT, Prud'homme RK, Ahl PL, Meers P, Kohn J. Association of hydrophobically-modified poly(ethylene glycol) with fusogenic liposomes. Biochim Biophys Acta 2003;616:184–95.
[46] Adamson P, Etienne S, Couraud PO, Calder V, Greenwood J. Lymphocyte migration through brain endothelial cell monolayers involves signaling through endothelial ICAM-1 via a rho-dependent pathway. J Immunol 1999;162:2964–73.
[47] Murciano JC, Muro S, Koniaris L, Christofidou-Solomidou M, Harshaw DW, Albelda SM, et al. ICAM-directed vascular immunotargeting of anti-thrombic agents to the endothelial surface. Blood 2003;101:3977–84.
[48] Muro S, Gajewski C, Koval M, Muzykantov R. ICAM-1 recycling in endothelial cells: a novel pathway for sustained intracellular delivery and prolonged effects of drugs. Blood 2005;105(2):650–8.
[49] Yang L, Kowalski JR, Yacono P, Bajmoczi M, Shaw SK, Froio RM, et al. Endothelial cell cortactin coordinates intercellular adhesion molecule-1 clustering and actin cytoskeleton remodeling during polymorphonuclear leukocyte adhesion and transmigration. J Immunol 2006;177:6440–9.
[50] Millan J, Hewlett L, Glyn M, Toomre D, Clark P, Ridley AJ. Lymphocyte transcellular migration occurs through recruitment of endothelial ICAM-1 to caveola- and F-actin-rich domains. Nat Cell Biol 2006;8:113–U115.
[51] Setiadi H, McEver RP. Clustering endothelial E-selectin in clathrin-coated pits and lipid rafts enhances leukocyte adhesion under flow. Blood 2009;111:1989–98.
[52] Leaver J, Alonso A, Durrani AA, Chapman D. The physical properties and photopolymerization of diacetylene-containing phospholipid liposomes. Biochim Biophys Acta 1983;732:210–8.
[53] Nino MRR, Lucero A, Patino JMR. Relaxation phenomena in phospholipid monolayers at the air–water interface. Colloids Surf Physicochem Eng Aspects 2008;320:260–70.